References

BATTERMAN, B. W. & COLE, H. (1964). *Rev. Mod. Phys.* **36**, 681.

BUCKSCH, R., OTTO, J. & RENNINGER, M. (1967). *Acta Cryst.* **23**, 507.

COLE, H. & STEMPLE, N. R. (1962). *J. Appl. Phys.* **33**, 2227.

HIRSCH, P. B. & RAMACHANDRAN, G. N. (1950). *Acta Cryst.* **3**, 187.

JAMES, R. W. (1950). *The Optical Principles of the Diffraction of X-rays*. London: Bell.

LAUE, M. VON (1960). *Röntgenstrahl-Interferenzen*. Frankfurt: Akad. Verlag.

MILLER, F. (1935). *Phys. Rev.* **47**, 209.

ZACHARIASEN, W. H. (1945). *Theory of X-ray Diffraction in Crystals*. New York: John Wiley.

Acta Cryst. (1971). A**27**, 284

A Neutron Fourier Chopper for Single Crystal Reflectivity Measurements: Some General Design Considerations*

BY A. C. NUNES

Brookhaven National Laboratory, Upton, New York 11973, *U.S.A.*

R. NATHANS

State University of New York, Stony Brook, New York 11790, *U.S.A. and Brookhaven National Laboratory, Upton, New York* 11973, *U.S.A.*

AND B. P. SCHOENBORN

Brookhaven National Laboratory, Upton, New York 11973, *U.S.A.*

(*Received* 16 *March* 1970)

Neutron single-crystal analysis of complex protein structures requires the collection of intensity data on a large number of reflections. The use of time-of-flight analysis (in particular Fourier time-of-flight analysis employing phase detection) of diffraction data, offers a significant increase in the efficiency of the use of reactor neutrons. Such a method would facilitate the use of neutron diffraction in protein structure work. In this paper, we investigate the use of the Fourier chopper in single-crystal work. We examine the effect of various system parameters (frequency stability, flight path fluctuations, collimation, sample mosaic spread, inaccuracy in phase detection, and statistical counting errors) and determine general specifications for such an apparatus. None of these specifications appears to be beyond present day technology.

1. Introduction

The use of neutron diffraction in structure studies of complex organic molecules is attracting the interest of crystallographers (Moore, Willis & Hodgkin, 1967; Schoenborn, 1969). Neutrons offer the following advantages: (1) hydrogen atoms become visible, (2) nitrogen atoms may be distinguished from carbon or oxygen atoms, (3) damage to specimens during irradiation is absent and (4) anomalous dispersion offers the possibility of easily phasing diffraction data. The chief disadvantage of neutrons is that compared with X-ray sources, the neutron flux (monochromated and collimated) available from even the highest flux reactors is down by a factor of 10^5 [as compared with a copper target rotating anode X-ray source (Arndt, 1969)].

Neutrons and neutron sources differ from X-rays and their sources in a number of additional ways. Neutron velocity is low (thermal neutron velocity is of the order of 2200 meter/second). The neutron source emits a Maxwellian distribution of velocities unlike the characteristic radiation of X-ray sources. In spite of these fundamental differences, present day neutron diffraction apparatus is basically identical to its X-ray counterpart. Typically, a narrow 'slice' of the reactor spectrum is selected by a crystal, providing a beam of monochromatic radiation which is then fed into a spectrometer equipped with a computer-controlled four-circle goniometer (Hamilton, 1968). Because this scheme of collecting data requires an essentially monochromatic beam, most of the source neutrons are wasted.

Other inefficiencies are built into this scheme. Data is taken sequentially, rocking the crystal through one reflection, then another, and so on. At any given time, typically less than one part in 10^6 of the neutrons striking the monochromator are detected at the counter.

* Work performed under the auspices of the U.S. Atomic Energy Commission,

We can make up for a large number of these inefficiencies by having the entire polychromatic beam strike the specimen crystal. The resulting Laue pattern would be composed of a number of spots, each of which is made up of the various orders of a particular class of reflections. The identity of the particular class can be established from knowledge of the unit cell, the detector position, and specimen crystal orientation. The intensity in the spot, *i.e.* the detector counting rate, is given by (Zachariasen, 1967)

$$I_{h,k,l}=\sum_{n=1}^{N}\Phi(\lambda/n)\frac{(\lambda/n)^4}{2\sin^2\theta}|F_{nh,nk,nl}|^2N_c^2\delta V \qquad (1)$$

where $\Phi(\lambda/n)$ is the incident neutron flux per unit wavelength at neutron wavelength λ/n, θ is the Bragg angle of the Laue spot, F is the reflection structure factor, N_c is the unit-cell density of the sample crystal and δV the volume of the sample. h, k, and l are the primary Miller indices of the Laue spot. The number of reflections 'N' observed in a single spot will be finite only if the incident spectrum is also finite.

The advantages of this arrangement over the conventional diffractometer are obvious. Full use is made of the entire reactor spectrum. No rocking of the crystal is necessary since the intensity in the diffracted beam is the integrated intensity (Lowde, 1956). Data can be taken at a large number of angles simultaneously, using a multidetector counting system. The main disadvantage of this technique, recognized by Lowde (1956) is its inability to separate the intensity of each spot into the individual integrated intensity data of the component orders. Without this separation, the technique is of little or no use in protein structure work.

As is shown in this report, we can achieve this separation by using a time-of-flight technique involving the sinusoidal modulation of the intensity of the incident beam. Thus, we can preserve the gain in data collection efficiency afforded by simultaneous use of nearly the entire reactor spectrum, and still obtain reliable measures of the integrated intensities in large numbers of Bragg reflections. The high transmission of a Fourier chopper (duty cycle $\simeq 25\%$ for a wheel and stator arrangement) allows a substantial incident intensity gain over the more conventional time-of-flight analysis described by Buras, Mikke, Lebech & Leciejewicz (1965).

The remainder of this paper consists of four sections, conclusions, and an Appendix. § 2 covers the mathematics of phase sensitive time-of-flight decomposition of a Laue spot. In this section, we also discuss the effects of uncertainties in the knowledge of the neutron flight time and modulation frequency. In § 3, we discuss resolution effects due to statistical uncertainties in frequency control and phase detection. § 4 describes how data are analyzed to yield integrated intensities and the uncertainty in each such intensity determination. § 5 sketches the value of combining the Fourier chopper with a multiple detector system. The Appendix presents the derivation of essential expressions discussed in the body of this paper.

2. Phase-sensitive analysis of a Laue spot

The time-of-flight neutron apparatus can best be treated, as shown by Colwell, Lenihan, Miller & Whittemore (1968), in the formalism of electronic circuit theory. The system is treated as a filter (or 'linear system' see Lee, 1966) whose transfer function is the time-of-flight spectrum. The spectrum of a Laue spot consists of a finite number of discrete peaks characterized by neutron transit times of τ, $\tau/2$, $\tau/3$, ... τ/N, ($\tau=\lambda\ l/3956$, where λ the neutron wavelength is in ångströms, l the flight path is expressed in meters, and τ in seconds) where N is the highest order allowed by the incident spectrum. When each order is infinitely sharp, this time-of-flight spectrum may be expressed as a sum over delta functions

$$f(t)=\sum_{n=1}^{N}I_n\delta(t-\tau/n)\,, \qquad (2)$$

where I_n is the integrated neutron intensity in the nth order reflection. If the intensity of the incident beam is mechanically modulated with rotational frequency ω, then we will have impinging on the sample a time varying intensity of the form

$$I_0(t)=1+A\sin(\omega t)+B\sin(2\omega t)+C\sin(3\omega t)+\ \ldots \qquad (3a)$$

where

$$A+B+C+\ \ldots\ =1 \qquad (3b)$$

Note that we have included a DC component, as neutron intensity can never be negative, and allowed for higher harmonics. The constant A lies between zero and one, and is determined by apparatus design (if, for example, our chopper consists of a wheel of identical radial slots rotating past a stator of similar design, A cannot be greater than 0·8 as the waveform produced is not a pure sinusoid). The effects of higher harmonics and the Fourier chopper have been considered by Colwell *et al.* (1968) and are not serious for the radial slot machine (sawtooth wave generator). In this paper, we consider higher harmonics in permitting A to take on values less than one, while otherwise ignoring them. In this approximation, the time dependent intensity seen by the detector will be

$$I(t)=\int_{X=-\infty}^{\infty}\sum_{n=1}^{N}I_n(1+A\sin\omega X)\delta\times(t-\tau/n-X)\mathrm{d}X+I_B \qquad (4)$$

which is

$$I(t)=\sum_{n=1}^{N}I_n\left\{1+A\left[\sin(\omega t)\cos\left(\frac{\omega\tau}{n}\right)-\cos(\omega t)\sin\left(\frac{\omega\tau}{n}\right)\right]\right\}+I_B. \qquad (5)$$

Here I_B is a constant background arising from general room background, and incoherent and/or inelastic pro-

cesses occurring within the sample itself. Note that equation (5) can be rewritten in the following form

$$I(t)=C+D\sin(\omega t+\varphi) \tag{6}$$

where, for any given Laue spot and fixed sample orientation, C is a constant while D and φ are functions of ω, τ, and the relative values of the I_n's.

The essentials of a single detector Fourier chopper system as described by Colwell *et al.* (1968) are depicted in Fig. 1. In this method of gathering data, the pulses from the detector are fed into four scalers, *a*, *b*, *c*, and *d*, each of which is activated during one quarter of a cycle of the incident modulation. After collecting data for a time T ($T\gg 1/\omega$) the scalers are read and the following functions constructed:

$$B = a+b+c+d \tag{7a}$$
$$C(\omega)=a-b-c+d \tag{7b}$$
$$S(\omega)=a+b-c-d\,. \tag{7c}$$

It is easy to show that these functions are equivalent to:

$$B=T\left(\sum_{n=1}^{N} I_n+I_B\right) \tag{8a}$$

$$C(\omega)=2(TA/\pi)\left(\sum_{n=1}^{N} I_n\cos(\omega\tau/n)\right) \tag{8b}$$

$$S(\omega)=-2(TA/\pi)\left[\sum_{n=1}^{N} I_n\sin(\omega\tau/n)\right] \tag{8c}$$

The constant B is simply the total number of neutrons collected in time T. It is necessary in scaling $C(\omega)$ and $S(\omega)$ and in determining the statistical uncertainty of these quantities. $C(\omega)$ and $S(\omega)$ are finite trigonometric series whose coefficients are the integrated intensities of the Bragg reflections of the Laue spot.

By taking data at a small number of properly chosen frequencies, one can obtain values of $C(\omega)$ and $S(\omega)$ associated with a set of independent equations which may be inverted to yield the I_n's. The minimum number of frequencies required to produce N such independent equations is just $N/2$ (or $N/2-1$ if N is odd). Although there are many other possible choices for our set of frequencies, we shall in this paper discuss only the case of the minimum sized frequency net.

By solving sets of equations of the above form, it can be shown that extremely small variations in τ produce large errors in the calculated values of the coefficients I_n, especially when n is large. While both frequency ω and time-of-flight τ enter the equations in the same way, frequency measurements accurate to one part in 10^5 are readily performed, and this accuracy is sufficient to introduce negligible error into the analysis. Such an independent determination of τ (from independent measurements of flight path and neutron wavelength) is, however, not feasible. We can, however, calculate τ precisely by collecting data for $N+1$ orders, and then analyzing our data for I_n and τ subject to the constraint that $I_{N+1}=0$. Since it is only the mean values of τ and ω which must be determined with this high accuracy, we do not see this precision as an important obstacle to the use of the technique.

3. Instrumental resolution

Additional variations in flight path and frequency during a measurement tend to smear out any time dependent intensity variations impressed on the neutron beam thus degrading data. Finite detector thickness, finite sample size, non-zero collimation and mosaic spread of the sample, and small irregularities in the drive speed of the chopper itself all contribute. Considering such fluctuations to be relatively small, and assuming a Gaussian shape to the time-of-flight spectrum peaks, it can be shown (see Appendix) that equations (8*b*) and (8*c*) become:

$$C(\omega)=(2TA/\pi)\sum_{n=1}^{N} I_n\cos(\omega\tau/n)\exp\left[-\tfrac{1}{2}(\omega\tau K/n)^2\right] \tag{9a}$$

$$S(\omega)=-(2TA/\pi)\sum_{n=1}^{N} I_n\sin(\omega\tau/n)\exp\left[-\tfrac{1}{2}(\omega\tau K/n)^2\right] \tag{9b}$$

where K is a constant of the form:

$$K=[(\delta\omega/\omega)^2+(\delta l/l)^2+(\delta\theta/\tan\theta)^2]^{1/2}\,. \tag{10}$$

Equation (8*a*) is unaffected. In the above, $\delta\omega/\omega$ and $\delta l/l$ are the fractional fluctuations in frequency and flight path respectively, θ is the Bragg angle of our Laue spot, and $\delta\theta$ is a measure of the total angular spread of the system consisting of both collimation and sample mosaic width. The constant K may be estimated

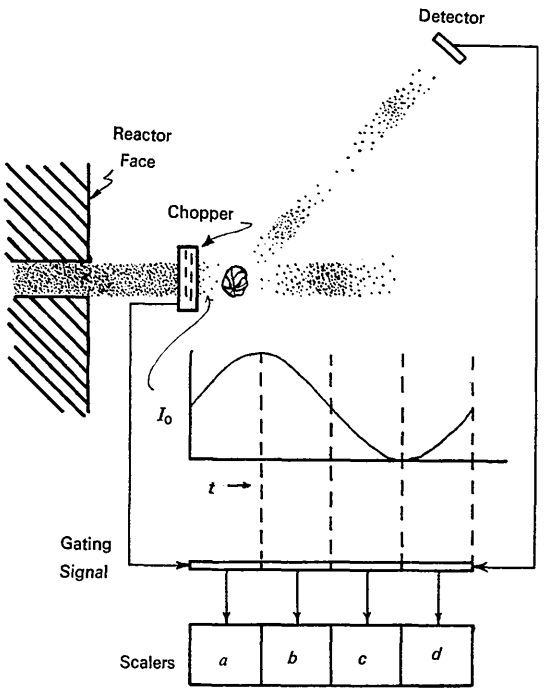

Fig. 1. A single detector Fourier chopper system.

from direct measurement of these instrumental parameters, or extracted from reflection data through use of equations (9*a*) and (9*b*).

The effects of possible error in detecting the exact phase of the chopper signal due to gating errors in the four signal scalers must also be considered. Four distinct gating signals must accurately define the four equal quadrants of the incident signal, and control the scalers accordingly. Errors in this mechanism can be of two types: (1) a statistical flutter of the gating signals about their correct phases, and (2) a constant displacement of one or all gating signals from their correct values.

The former merely enters as a frequency fluctuation, and can be directly included in the quantity, $\delta\omega/\omega$. If $\delta\varphi$ is the standard deviation of the flutter of a gating signal, and $(\delta\omega/\omega)_m$ is the actual fractional frequency flutter of the chopper mechanism, then

$$(\delta\omega/\omega)=[(\delta\omega/\omega)_m^2+(2\delta\varphi/\pi)^2]^{1/2}\,. \tag{11}$$

With existing electronics, such phase fluctuations can be held to a fraction of a per cent.

A constant bias in one or all of these gating signals will effectively change the values of $C(\omega)$ and $S(\omega)$ which are measured. If $\delta\varphi_b$ is a measure of this bias for all four gates, we can expect these changes in $C(\omega)$ and $S(\omega)$ to be of magnitude:

$$\delta S(\omega)\simeq\delta C(\omega)\simeq B\delta\varphi_b/2\pi\,. \tag{12}$$

With careful construction of equipment, one can expect to hold $\delta\varphi_b/2\pi$ below one per cent, rendering $\delta S(\omega)$ and $\delta C(\omega)$ from this source to be less than the statistical counting errors involved in data collection.

The statistical uncertainty involved in counting random events enters our analysis in a simple way. Assuming Poisson statistics, the uncertainty in $C(\omega)$ and $S(\omega)$ in any experiment will be simply equal to $(B)^{1/2}$. The uncertainties in $C(\omega)$ and $S(\omega)$ due to these effects are uncorrelated, thus one may perform calculations with combinations of $C(\omega)$ and $S(\omega)$ carrying the uncertainties along in the usual way. The uncertainties due to a phase bias, however, will generally be correlated, and a correct error analysis including them is rather complicated. Since they are expected to be small compared with $(B)^{1/2}$, we will neglect them here.

From the above analysis, it is clear that while the effects of instrumental resolution are not likely to be negligible, they can be treated in a straightforward manner. Thus, a useful chopper system can be constructed to mechanical and electronic tolerances easily obtainable by present day technology.

4. Data analysis

The crystallographic data we seek are the relative values of the integrated intensities I_n. We must therefore determine how uncertainties in $C(\omega)$ and $S(\omega)$ propagate through our analysis so as to be able to determine the uncertainty in any value of I_n we might calculate. We assume λ and τ to be approximately known from experimental geometry and the previously determined (perhaps by X-ray work) unit cell of our crystal.

With the availability of large general purpose digital computers, the simplest method of obtaining the intensities of the various orders is probably that of solving our set of independent simultaneous equations by determinants. We discuss the properties of this analysis technique here. If Δ is the determinant of our set of equations

$$\Delta=\begin{vmatrix} X_{1,1}X_{1,2}\ldots X_{1,N} \\ X_{2,1}X_{2,2}\ldots \\ \cdot \\ \cdot \\ X_{N,1}X_{N,2}\ldots X_{N,N} \end{vmatrix} \tag{13}$$

where

$$X_{i,n}=\begin{cases} (2(T_i)A/\pi)\cos(\omega_i\tau/n)\exp[-\frac{1}{2}(\omega_i\tau K/n)], & i\leq N/2 \\ -(2(T_{i-N/2})A/\pi)\sin(\omega_{i-N/2}\tau/n) & \\ \qquad \exp[-\frac{1}{2}(\omega_{i-N/2}\tau K/n)], & i>N/2 \end{cases} \tag{14}$$

and $\Delta_{i,n}$ is the cofactor of Δ associated with the (i,n)th element, then we can write:

$$I_n=\sum_{i=1}^{N/2}C(\omega_i)\,(\Delta_{i,n}/\Delta)+\sum_{i=N/2+1}^{N}S(\omega_{i-N/2})\,(\Delta_{i,n}/\Delta)\,. \tag{15}$$

Once we have accurately determined τ, and correctly measured other instrumental parameters (ω_i and K) the major source of uncertainty in the intensities I_n will be that introduced by statistical counting errors in $C(\omega)$ and $S(\omega)$. We can see how these errors affect the I_n's by taking the partial derivatives:

$$\partial I_n/\partial C(\omega_i)=(\Delta_{i,n}/\Delta), \qquad i\leq N/2 \tag{16a}$$

$$\partial I_n/\partial S(\omega_{i-N/2})=(\Delta_{i,n}/\Delta) \quad i>N/2 \tag{16b}$$

Since the errors of $C(\omega)$ and $S(\omega)$ are statistically uncorrelated, and Gaussian distributed with standard deviation equal to $(B_i)^{1/2}$, then the I_n's are also Gaussian distributed with standard deviation:

$$\delta I_n=\left|\sum_{i=1}^{N/2}B_i(\Delta_{i,n}/\Delta)^2+\sum_{i=N/2+1}^{N}B_{i-N/2}(\Delta_{i,n}/\Delta)^2\right|^{1/2}. \tag{17}$$

The uncertainty in our intensities then is a rather complicated function of our set of frequencies, the first order flight time of our neutrons, and the time spent collecting data at any frequency. A well designed experiment will be one which chooses ω_i,τ, and T_i to minimize $\delta I_n/I_n$. This optimization is generally only possible when the I_n's are already known. Although this is never the case, one may obtain some knowledge of the integrated intensities beforehand by rapidly scanning through the reflections, or guessing a structure

from data available and calculating expected intensities. Either or both of these approaches will allow one to establish some criterion for optimizing these experimental parameters.

When one has little previous knowledge of the intensities I_n, one may choose all T's to be equal. In this case, the values of ω_i and τ which minimize the δI_n's are those for which the determinant of the equations is an extremum. The uncertainties in the I_n's increase as we change $\omega_i\tau$ to produce non-extremum values of Δ, and approach infinity when Δ goes to zero (*i.e.* where the equations are either no longer independent, or where they become a homogeneous set, in which case determinant solutions are not possible). This is illustrated in the following computer simulation of a Fourier chopper experiment.

We have assumed a chopper system in which $K=0{\cdot}02$, and where formulae (9*a*) and (9*b*) apply. We assume that the Laue spot of interest consists of only first, second, and third orders of respective intensities 10000, 1000, and 100 neutrons per unit time $T=\pi/2A$. We have left $I=0$, so as to allow for the determination of τ from our data, employing a net of only two different frequencies. Assuming $A\simeq 0{\cdot}8$, and a background roughly 10% of the elastic intensity, we calculate $(B)^{1/2}=155$. We have calculated $\delta I_n/I_n$ for a few combinations of $\omega_i\tau$, and present the results in Table 1. (One can get a feel for the magnitude of the frequencies involved by assuming that the first order neutron is of 3 Å wavelength, and that the flight path is one meter. The first order transit time is the 0·758 milliseconds, and the frequency corresponding to $\omega\tau=2\pi$ is just $=8{\cdot}205$ radians/sec or $f=\omega/2\pi=1{\cdot}32$ kHz, which is relatively low.)

We see from Table 1 that $\delta I_n/I_n$ is generally minimal where Δ is an extremum. Fig. 2 presents a plot of the absolute value of Δ as a function of $\omega_1\tau$ and $\omega_2\tau$. At points of extreme Δ, the values of δI_n are roughly the same for all orders, rendering the weakest order indistinguishable from background. In no case is the weakest reflection detected. This is the most serious limitation of the Fourier method. If accurate measurement of the intensity of weak reflections is essential, one can take some advantage of the shape of the incident spectrum and orient the sample to maximize the weaker orders and minimize the strong, or alternatively one may simply measure such weak reflections on a more conventional spectrometer.

In protein structure studies, the general practice is to measure many more reflections than are strictly required, thus overdetermining the structure. This is done, in part, to help correct for inaccuracies in each individual reflectivity determination. In this type of work, we expect that the ability of the Fourier chopper system to rapidly measure a large number of reflections will far outweigh its inability to precisely measure the weakest reflections.

Since the above analysis depends upon the finiteness of the number of orders in a Laue spot, it may prove

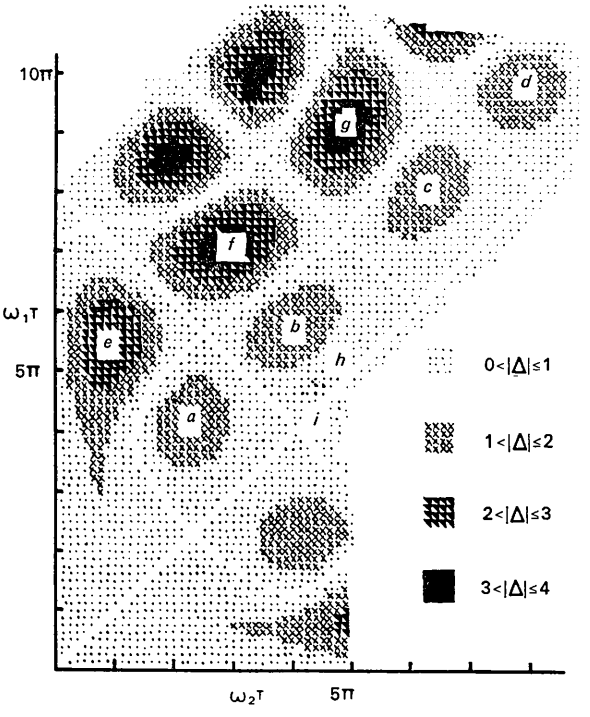

Fig. 2. Absolute value of the four by four determinant used in analyzing the three-order Laue spot as a function of $\omega_1\tau$ and $\omega_2\tau$.

Table 1. *Some values of* $\delta I_n/I_n$ *calculated for the Fourier decomposition of a three-order Laue spot assuming* $I_n=10000$, 1000, 100 neutrons/T *respectively,* $T=\pi/2A$, $A=0{\cdot}8$, $K=0{\cdot}02$, *and* $I_B=1000$ neutrons/T

Position code (Fig. 2)	$\omega_1\tau$	$\omega_2\tau$	Determinant extremum?	$\delta I_1/I_1$	$\delta I_2/I_2$	$\delta I_3/I_3$
a	13·35	7·069	yes	0·012	0·063	0·56
b	18·06	12·17	yes	0·013	0·19	1·93
c	25·53	19·63	yes	0·015	0·204	2·26
d	30·63	24·35	yes	0·014	0·115	1·30
e	17·24	2·75	yes	0·012	0·16	1·42
f	22·38	9·032	yes	0·012	0·26	1·21
g	28·67	15·31	yes	0·015	1·01	2·37
h	16·08	14·92	no	0·028	0·69	4·59
i	12·96	13·75	no	0·044	0·53	4·50

necessary to sharply terminate the incident beam spectrum at both long and short wavelength limits. A certain amount of filtering is necessary anyway to eliminate ionizing radiation from the beam to prevent sample damage, and to control the number of Laue spots to prevent overlap of one spot upon another,

In determining any structure, we require the relative intensities of the various Bragg reflections. This means that we must normalize all intensities to account for the variation in the incident intensity with wavelength. For this a knowledge of the reactor spectrum and its variation with time is required. This may be accomplished with another crystal (of known reflectivity) and another detector making use of the same chopper for time-of-flight analysis.

Some crystal parameters are also wavelength dependent, and must be determined before accurate structure factors can be calculated. Such parameters include neutron attenuation by the sample, and possible extinction effects within the sample.

For the sake of illustration, only three orders were assumed above. In an actual experiment with a complicated protein crystal, one would expect to see up to thirty or forty orders in high symmetry directions. In this case, the computations become more lengthy, but are identical in form to those employed above.

5. A multidetector Fourier chopper

The great attractiveness of the Fourier chopper lies in its adaptability to a multidetector system. A number of promising multiple detector and position sensitive detector systems ultimately adaptable to neutron work are presently under development at Brookhaven (Thomas & Hamilton, 1969), Oak Ridge (Borkowski & Kopp, 1968; Davidson, 1968), and other laboratories.

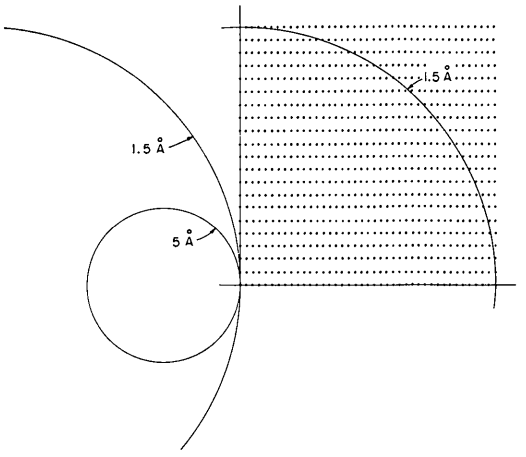

Fig. 3. One quadrant of a basal plane of the reciprocal lattice of a hypothetical protein crystal with cell dimensions 30 × 60 Å, and the limiting Ewald spheres of the neutron spectrum. All reflections falling between the two spheres are in reflecting positions. With a large bank of detectors, relatively few crystal orientations are needed to obtain data for a 1·5 Å resolution structure determination.

Fig. 3 represents part of a protein crystal reciprocal-lattice layer, and the limiting Ewald spheres for a neutron spectrum of 1·5 to 5 Å. In high symmetry directions, one may observed up to 30 or 40 orders in a Laue spot, though the average number of orders per spot will be much lower, perhaps three or four. The crystal, mounted on an on-line computer-controlled three-circle goniometer will be oriented to maximize the data collection efficiency of the detector array.

6. Conclusions

The above analysis has demonstrated how a Fourier chopper might be applied to the problem of gathering neutron diffraction data for single crystal protein structure work. None of the problems foreseen in the design of such a system is insoluble by today's technology. Such a system appears to be mechanically and electronically relatively simple yet potentially extremely economic of reactor neutrons (a multidetector Fourier chopper system being 100 to 1000 times more efficient than a conventional spectrometer). Though limitations exist in the ability of such a system to measure very weak reflections in the presence of strong ones, it should be eminently capable of gathering vast amounts of data on a large number of reflections in a short time. This makes such a system very attractive for protein structure work in which one generally tries to overdetermine the structure by measuring more reflections than is absolutely necessary. Maximum efficiency of such a system requires the services of a moderate sized (off-line) computer (50,000 core locations), in addition to a smaller on-line machine.

A Fourier chopper system is now under construction at Brookhaven National Laboratory for evaluation at the High Flux Beam Reactor.

The authors are grateful to Dr W. L. Whittemore of Gulf General Atomic for a number of discussions regarding the applications of the Fourier chopper. We also wish to thank Miss Nancy Chesser for writing the computer programs used in this study.

APPENDIX

We shall here sketch the derivation of formulae (9*a*), (9*b*) and (10), and determine their range of applicability. In this derivation, we will consider two independent sources of instrument error: that introduced by statistical variations in neutron transit time, and frequency instability in the chopper itself.

Since a neutron may be diffracted from any region of the sample crystal, and detected in any part of the active region of the detector, no two neutrons will have exactly the same flight path. The actual flight path of any neutron will vary about a mean value l with a standard deviation δl, which will be roughly equal to the

sum of sample and detector thickness. The fractional uncertainty in neutron transit time due to this effect will be

$$\delta\tau/\tau|_l=\delta l/l\,. \tag{18}$$

Due to finite collimation of the incident beam, and finite mosaic spread of the sample, the actual neutron scattering angle will fluctuate about the mean Bragg angle θ_B with a standard deviation δ_θ. This implies a spread in wavelengths of the Bragg reflected neutrons, with a resulting fractional uncertainty in transit time of

$$\delta\tau/\tau|_\theta=\delta\theta/\tan\theta_B\,. \tag{19}$$

The above effects are independent. If we assume both to introduce a Gaussian spread of neutron transit times, then the time-of-flight distribution of a Laue spot will be

$$f(t)=\sum_{n=1}^{N} I_n \frac{\exp\left\{-\frac{1}{2}\left(\frac{t-\tau/n}{K_\tau\tau/n}\right)^2\right\}}{\sqrt{2\pi}(K_\tau\tau/n)}, \tag{20}$$

where

$$K_\tau=\sqrt{\left(\frac{\delta l}{l}\right)^2+\left(\frac{\delta\theta}{\tan\theta_B}\right)^2}\,. \tag{21}$$

The time dependent counting rate seen by the detector, when the incident beam is sinusoidally modulated ($I_0=1+A\sin\omega t$), is

$$I(t)=\int_{\infty}^{t}\sum_{n=1}^{N}[1+A\sin(\omega X)]I_n \times\frac{\exp\left\{-\frac{1}{2}\left(\frac{t-\tau/n-X}{K_\tau\tau/n}\right)^2\right\}}{\sqrt{2\pi}(K_\tau\tau/n)}\,dX+I_B \tag{22}$$

where once again, I_B is the system background counting rate. For reasons of causality, the limits of integration on both equations (22) and (4) should be $-\infty$ to t. Since t is always taken to be very much larger than the time-of-flight 'τ/n' and the width of the time-of-flight distribution $K_\tau\tau/n$, we have made the approximation of integrating to $+\infty$ to obtain

$$I(t)=\sum_{n=1}^{N} I_n\left[1+A\exp\left\{-\frac{1}{2}\left(\frac{\omega\tau K_\tau}{n}\right)^2\right\} \times\left(-\sin\frac{\omega\tau}{n}\cos\omega t+\sin\omega t\cos\frac{\omega\tau}{n}\right)\right]+I_B. \tag{23}$$

By collecting data in four-gated scalers, each scaler contains the time-integrated intensity in one quadrant of the incident oscillation. Performing this time integration, and forming the appropriate sums and differences we have, after collecting data for a total time T:

$$B=T\left|\sum_{n=1}^{N} I_n+I_B\right| \tag{24a}$$

$$C(\omega)=+\frac{2AT}{\pi}\times\sum_{n=1}^{N} I_n\exp\left\{-\frac{1}{2}\left(\frac{\omega\tau}{n}K_\tau\right)^2\right\}\cos\left(\frac{\omega\tau}{n}\right) \tag{24b}$$

$$S(\omega)=-\frac{2AT}{\pi}\times\sum_{n=1}^{N} I_n\exp\left\{-\frac{1}{2}\left(\frac{\omega\tau}{n}K_\tau\right)^2\right\}\sin\left(\frac{\omega\tau}{n}\right). \tag{24c}$$

The smearing of the transit time has reduced the effective magnitude of I_n by the above exponential factor.

If we now allow the chopper frequency to vary in a Gaussian way about a mean frequency ω, the measured value of B does not change, but the values of $C(\omega)$ and $S(\omega)$ will be the above functions averaged over the distribution:

$$P(\omega_x)d_x=\frac{\exp\left\{-\frac{1}{2}\left(\frac{\omega_x-\omega}{\omega K_\omega}\right)^2\right\}}{\sqrt{2\pi}\omega K_\omega}\,d\omega_x\,, \tag{25}$$

where

$$K_\omega=\delta\omega/\omega \tag{26}$$

is the fractional standard deviation of the distribution. Performing the average, we have

$$\langle C(\omega)\rangle=+\frac{2TA}{\pi}\sum_{n=1}^{N} I_n\frac{\cos\frac{\omega\tau/n}{1+\varepsilon^2}}{\sqrt{1+\varepsilon^2}}\exp\left\{-\frac{1}{2}\left|\frac{K^2(\omega\tau/n)^2}{1+\varepsilon^2}\right|\right\} \tag{27a}$$

$$\langle S(\omega)\rangle=-\frac{2TA}{\pi}\sum_{n=1}^{N} I_n\frac{\sin\frac{\omega\tau/n}{1+\varepsilon^2}}{\sqrt{1+\varepsilon^2}}\exp\left\{-\frac{1}{2}\left|\frac{K^2(\omega\tau/n)^2}{1+\varepsilon^2}\right|\right\} \tag{27b}$$

where we have set

$$\varepsilon=K_\omega K_\tau\omega\tau/n \tag{28}$$

and

$$K^2=K_\tau^2+K_\omega^2\,. \tag{29}$$

Equation (29) is simply equation (10) in slightly different form. When $\varepsilon<0{\cdot}1$, the above formulae approach the forms (9*a*) and (9*b*).

Let us now determine how large ε might be for a working apparatus. If we have a system with a one-meter flight path, a 5 mm thick detector, and a sample crystal also of 5 mm dimensions, we shall have:

$$\delta l/l\lesssim 0{\cdot}01$$

If we restrict our scattering angle to be greater than 5°, and assume that collimation and sample mosaic combine to produce $\delta\theta\simeq 0{\cdot}5°$, then we will have

$$\delta\theta/\tan\theta_B\lesssim 0{\cdot}1\,,$$

and

$$K_\tau\lesssim 0{\cdot}1\,.$$

Let us assume a frequency stability of

$$K_\omega = 10^{-3} .$$

If our top frequency in 50 kHz, and the longest wavelength we detect is 10 Å, we will have $\omega\tau/n \lesssim 794$, and

$$\varepsilon \simeq 0{\cdot}08 .$$

Such a chopper system would be adequately described by equations (9*a*) and (9*b*).

References

ARNDT, U. W. (1969). Private communication.

BORKOWSKI, C. J. & KOPP, M. K. (1968). *Rev. Sci. Instrum.* **39**, 1515.

BURAS, B., MIKKE, K., LEBECH, B. & LECIEJEWICZ, J. (1965). *Phys. Stat. Sol.* **11**, 567.

COLWELL, J. F., LENIHAN, S. R., MILLER, P. H. JR & WHITTEMORE, W. L. (1968). *Fourier Analysis of Thermal Neutron Time-of-Flight Data: A High Efficiency Neutron Chopping System*, Gulf General Atomic GA-9110.

DAVIDSON, J. B. (1969). *Acta Cryst.* A**25**, S66.

HAMILTON, W. C. (1968). *J. Comp. Phys.* **2**, 417.

LEE, Y. W. (1966). *Statistical Theory of Communication*, pp. 323–351. New York: John Wiley.

LOWDE, R. D. (1956). *Acta Cryst.* **9**, 151.

MOORE, F., WILLIS, B. T. M. & HODGKIN, D. C. (1967). *Nature, Lond.* **214**, 130.

SCHOENBORN, B. P. (1969). *Nature, Lond.* **224**, 143.

THOMAS, R. & HAMILTON, W. C. (1969). *Acta Cryst.* A**25**, S69.

ZACHARIASEN, W. H. (1967). *Theory of X-ray Diffraction in Crystals*, pp. 105–106. New York: Dover.

Acta Cryst. (1971). A**27**, 291

Absorption and Volume Corrections for a Cylindrical Sample, Larger than the X-ray Beam, Employed in Eulerian Geometry

BY B. A. COYLE* AND L. W. SCHROEDER†

Department of Chemistry and the Materials Research Center, Northwestern University, Evanston, Illinois 60201, *U.S.A.*

(*Received* 1 *June* 1970)

A treatment of the absorption and volume corrections for a cylindrical sample, which is larger than the X-ray beam and which is employed in 'Eulerian cradle' geometry, is described. The procedure described here is strictly correct only for a one-dimensional X-ray beam, but it has given satisfactory results for a beam of finite cross section. The calculation is easily done by computer and requires only the radius of the sample, the 2θ and χ values for each reflection, and the zeros of Legendre polynomials and their weights if Gaussian integration is used.

Introduction

Although procedures for absorption corrections have been extended to crystals of arbitrary shape and to diffraction geometries currently in use, most of these treatments assume that the crystal is completely irradiated by the primary X-ray beam (see, for example, Wuensch & Prewitt, 1965). However, Skertchly (1957) has pointed out that in the investigation of metallic and fibrous substances it is often convenient to use a cylindrical specimen having a diameter larger than that of the X-ray beam. He treated the case of a cylindrical specimen irradiated with a fine beam at perpendicular incidence.

A situation arose in our laboratory involving a large cylindrical crystal and 'Eulerian cradle' geometry (Coyle, Schroeder & Ibers, 1970) where the incident beam and the crystal are not necessarily perpendicular. An absorption and volume correction for such a geometry is developed in this paper. The treatment developed is subject to two limitations. A minor restriction is that the axis of the cylindrical crystal be coincident with the φ (polar) axis of the 'Eulerian cradle' (Furnas, 1957). This should be easily achieved in most experimental situations. The second limitation is that our treatment is exact only for a one-dimensional beam. Thus, it is desirable that the ratio of the beam diameter to the diameter of the cylinder be as small as is experimentally feasible.

When a crystal is not totally bathed in an X-ray beam the volume of that crystal seen by the beam is not necessarily constant for various reflections, and the amount of variation depends on the geometry of

* Present address: Department of Chemistry, North Central College, Naperville, Illinois, U.S.A.

† Present address: Center for Radiation Research, National Bureau of Standards, Washington, D.C., U.S.A.